

Scatter radiation dose profile evaluation in computed tomography using Monte Carlo simulation

Gh.R. Fallah Mohammadi^{1*}, L. Hesamnezhad², M. Mahdavi²

¹Department of Radiology, Faculty of Allied Medicine, Mazandaran University of Medical Sciences, Sari, Iran

²Department of Physics, University of Mazandaran, Babolsar, Iran

ABSTRACT

Background: Conventional radiation dosimetry methods in computed tomography (CT) are not able to measure the dose distribution along the patient's longitudinal axis. To calculate the dose index on a CT scan, the dose distribution from the center of the radiation field must be calculated. In this study, the most appropriate integral interval for calculating the CT dose index in the axial mode was determined using the Monte Carlo (MC) method based on X-ray photon energy and slice thickness. **Materials and Methods:** The computed tomography dose index (CTDI) phantom was simulated in the EGSnrc/BEAMnrcMC system and was irradiated with several X-ray energies and several slice thicknesses and dose profiles in phantom were investigated. The area under the dose profile and the scatter to primary radiation dose ratio (SPR) were calculated. **Results:** The range of scattered beams from the center of the radiation field reaches 450 mm in 140 kV and a 40 mm slice thickness. The SPR value for all levels of X-ray photon energy (between 80 and 140 kV) significantly decreases as slice thickness increases. CT scan imaging technical factors greater than 310 mm from the center of the slice thickness have no effect on the behavior of the scattered radiation. **Conclusion:** The primary beams are more affected by the energy of the photons, and the scatter beams are more strongly affected by the slice thickness. For 64-slice scanners, the polymethyl methacrylate (PMMA) phantom length should be between 700 mm and 900 mm to yield accurate CTDI estimations.

Keywords: Dose profile, CT scan, scatter radiation, CTDI phantom, MC simulation.

INTRODUCTION

With the advent of multi-detector computed tomography (CT) and the use of narrow X-ray beams, it is necessary to study dosimetry and investigate the contribution to scatter radiation in soft tissue equivalent phantoms. Conventional dosimetry methods for CT scans are not able to measure the dispersion and distribution of the radiation dose along the long axis of the patient's body, and this lack of computation of the actual dose distribution leads to a dose underestimation in advanced CT scan systems⁽¹⁾. To estimate the proper dose in a CT scan, a computed tomography dose index (CTDI) is calculated using a dosimeter with 100 mm in

length (CTDI100), which is widely disagreed within many articles⁽²⁾. New standards are needed to accurately estimate patient doses in high-speed and wide-radiation beams in modern CT scan systems. One of these considerations is the length (i.e., the range of integral dose profile) of the CTDI phantom to determine the dose distribution of the scatter radiation along the central axis of the phantom. In a CT scan, the patient's dose from the scattered radiation is significant, reaching more than 14 times the initial beam at the center of the polymethyl methacrylate (PMMA) phantom with a diameter of 32 cm at 60 kV⁽³⁾. In order to accurately measure the patient dose, the behavior of scattered radiations inside the body must be

carefully monitored, and the dose spread from the central point of the slice thickness must be carefully measured. Given the high dose rate of CT scans, many efforts are being made to reduce the doses given to adult patients and children^(4, 5). Due to the increasing speed of CT scanners and their increasing clinical applications and widespread use—especially in children—dose reduction strategies are strongly considered⁽⁶⁾. When the X-ray beam width is increased, especially in multi-slice CT systems that emit a cone geometry beam from the X-ray tube, scattered photons have a greater role in reducing image quality and increasing patient dose⁽⁷⁻⁹⁾. One of the most important dosimeter tools is the Monte Carlo (MC) simulation method, in which the correct dosage calculation is possible for any desired environment. An accurate understanding of the dose distribution of scattered beams in the patient body equivalent phantom and how it changes with energy and slice thickness yields exact dose calculations and solutions that reduce the dose. Although ionizing chambers with a length of 300 mm have been used to increase the measurement range along the z-axis, this method is expensive, fragile, and heavy; thus, it is unsuitable for practical measurements and clinical use⁽¹⁰⁾. In this study, we simulated CTDI phantoms of 1000 mm in length using MC simulation. By doing this, we calculated the scatter radiation dose profile in the central axis of a phantom to estimate the best integral interval for calculating the CT scan dose index in an axial mode. The scatter radiation dose profile range changes with X-ray photon energy and radiation field slice thickness were also evaluated.

MATERIALS AND METHODS

In this study, the dose profiles of X-ray photons in CT scan imaging in a PMMA cylindrical phantom were investigated. An EGSnrc / BEAMnrc simulation code was used to simulate a GE-Light Speed CT system, 64 slices, manufactured by GE Healthcare Technologies (Waukesha, WI) in axial CT data acquisition

mode. The validity of this simulation code has been investigated in previous studies⁽¹¹⁾. The geometrical characteristics of the CT scan system and its hardware were simulated using existing tools of the BEAMnrc code.

The components of the CT scanner, including the X-ray tube, aluminum filters, bowtie shaping filters, and collimators, were simulated using the tools defined in the simulation code as the component module (CM). Two phase-space files (from the BEAMnrc code output files) were defined (one before the center and the other at the center of CT scan gantry). This file contains the history of all the particles generated in the simulation code. The BEAMnrc simulation code was developed to create phase-space files for X-ray photon energies of 80, 100, 120, and 140 kV and for slice thicknesses of 5, 10, 20, and 40 mm.

The X-ray photon energy and slice thickness were selected based on the most common technical parameters in CT scan imaging. In our study, 5×10^8 particles were irradiated to the phantom based on the equilibrium of the Monte Carlo simulation run time and acceptable measurement error⁽¹²⁾. In the Monte Carlo code, all the conditions for low-energy dose calculations were activated. BEAM Data Processor (BEAMDP) software was used to draw the particle flux as well as the energy distribution of the phase-space files. The DOSXYZnrc code was used to simulate the PMMA phantom (32 cm in diameter and 10 cm in length), irradiate the phantom, and evaluate the dose per voxel in the phantom. DOSCTP software was used to evaluate the 3ddose file (DOSXYZnrc code output file)⁽¹³⁾. In this file, the dose values per voxel of the phantom are stored. In order to study the dose profile, the range of scattered radiations was calculated up to the tenth and hundredth of the largest dose in slice thickness. The area under the dose profile curve of scattered and primary radiations, as well as the scatter to primary radiation dose ratio (SPR), were also calculated. Figure 1 shows a geometric view of the irradiation to the phantom in the simulation code.

The dose value of the center of the radiation field was calculated by varying the slice

thickness (mm) and energy of the X-ray photons (kV). The effect of these quantities on the dose profile at the central axis of the phantom was also investigated. The best integral interval for

calculating the CT scan dose index was introduced. EXCEL software was used to draw the dose profiles. Data were analyzed using descriptive statistics.

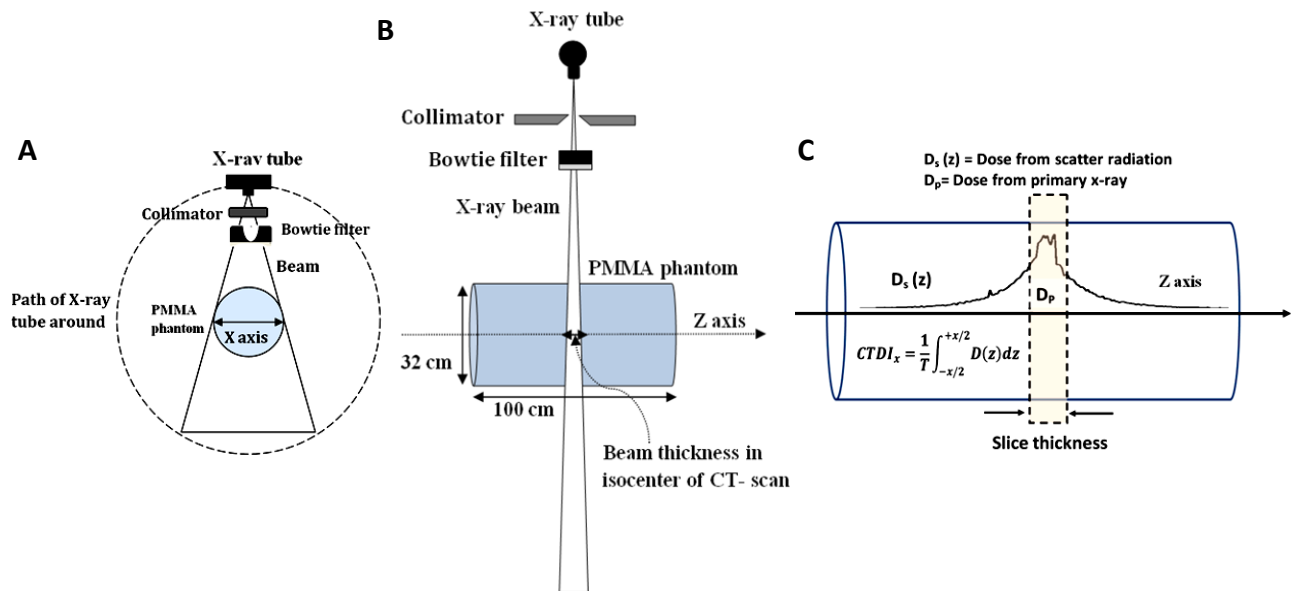


Figure 1. Irradiation geometry of the PMMA phantom in a CT scan system as axial mode **A**: front view. **B**: lateral view. **C**: dose profile in z-axis of the PMMA phantom.

RESULTS

In figure 2, several dose profiles of the scattered and primary radiations in the phantom (extracted from the information contained in the 3ddose file from DOSXYZnrc code outputs), as well as the X-ray photon flux distribution at the center of the CT scan gantry in the air (extracted

from the EGSPHSP file of the outputs of the BEAMnrc code), is shown along the Z-axis for several energy levels and slice thicknesses.

The dose was obtained at the center of slice thickness ($Z=0$) in the simulation code at the mentioned energy levels and slice thicknesses (figure 3).

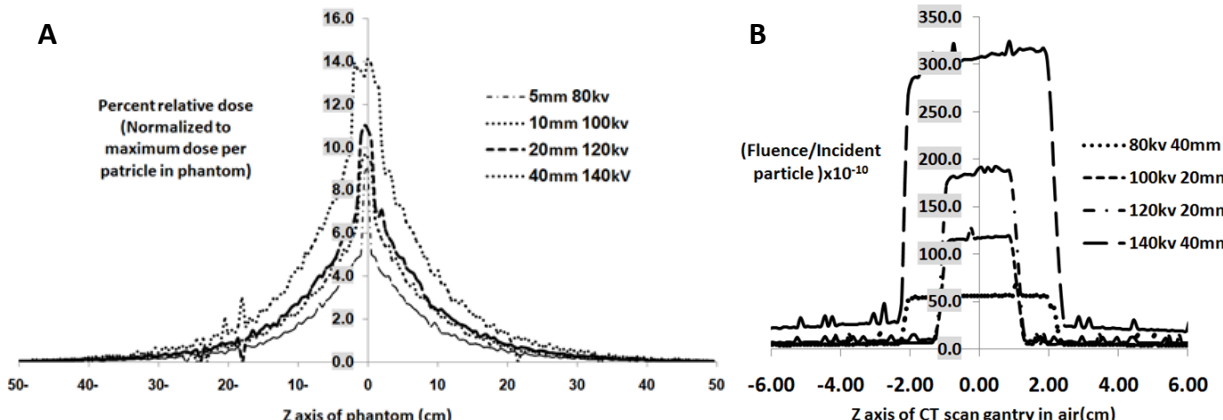


Figure 2 **A**. Dose distributions inside the PMMA cylindrical phantom (100 cm in length and 32 cm in diameter) at multiple energy levels and slice thickness. **B**. X-ray photon flux in the air in the isocenter of the CT system gantry along the slice thickness.

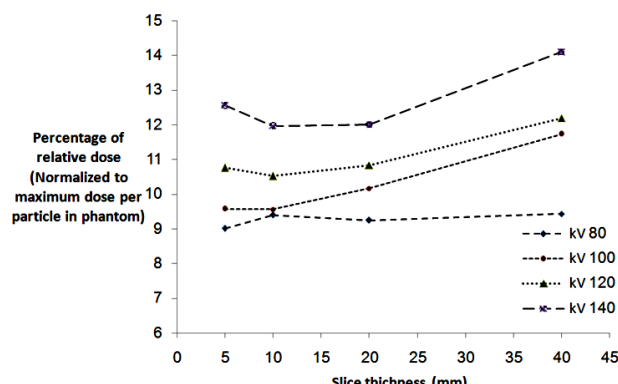


Figure 3. Changes in radiation dose at the center of the slice thickness with photon energy (kV) and the slice thickness (mm).

One of the most important parameters in the evaluation of the dose profile is the dose ratio of the scattered radiation to the primary radiation. By calculating the area under the curve of the dose profile for primary (D_p) and secondary (D_s) radiations, SPR was obtained at different slice thicknesses and photon energy levels. Figure 4 shows the SPR diagram.

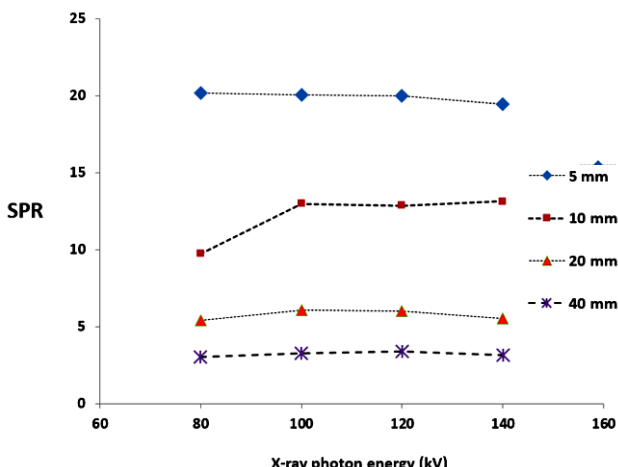


Figure 4. changes in SPR with X-ray energy and slice thickness (mm).

Much of the area under the dose profile curve belongs to scattered radiations. The range of scattered beams from the center of the radiation field depends on the X-ray photon energy and slice thickness. This value is an important consideration in the accurate computation of the CT dose index. Figure 2A shows the range of scattered photons from the central point of the slice thickness. In this study, to calculate the area under the dose profile curve, the range of scattered beams to the point where the dose

reaches one-hundredth of the dose value at the central axis of the slice was considered. Table 1 shows the range of scattered radiation at a distance where the dose value reaches one-tenth and one-hundredth of the maximum dose in the slice thickness.

Table 1. Range of scattered radiation (mm) as a function of X-ray photons energy (kV) and slice thickness (mm) along the Z-axis of the CTDI phantom in the positive direction of the axis up to one-tenth and one-hundredth of the maximum dose in the center of slice.

Dose limit	X-ray photon energy (kV)							
	80		100		120		140	
	a	b	a	b	a	b	a	b
Slice thickness (mm)	5	138 ±8	348 ±13	150 ±10	378 ±13	158± 13	375 ±10	155 ±10
	10	148 ±8	358 ±12	175 ±10	395 ±20	180 ±10	388 ±13	185± 10
	20	165 ±10	368 ±20	168 ±13	375 ±10	173 ±13	380 ±15	168 ±8
	40	177 ±15	387 ±12	188 ±13	395 ±20	195 ±15	418 ±13	200 ±10

a = one-tenth of the maximum dose in slice thickness.

b = one-hundredth of the maximum dose in slice thickness.

According to figure 2, the range of the scatter radiations can be calculated to a distance from the center of the slice thickness where the difference between the maximum and the minimum dose is significant. Table 2 shows the distance from the center of the slice, where the dose difference between the maximum energy (140 kV) and the minimum energy (80 kV) reaches zero. The values in table 2 are important because, beyond the stated distance, changes in the technical parameters do not affect the dose value of the scattered radiations.

Table 2. The distance (mm) from the center of the slice where the dose difference between the maximum energy (140 kV) and the minimum energy (80 kV) reaches zero.

Slice thickness (mm)	5	10	20	40
Scatter range (mm)	290	285	271	310

DISCUSSION

The photon flux profile is limited to the primary beams at the slice thickness. In very low-density materials such as air, the interaction of photons is very low, and therefore, less scattered radiation is produced (figure 2B). However, in

materials with a density similar to that of water (e.g., PMMA, muscle, blood, and solid tissues), the highest percentage of scattered radiation occurs ⁽¹⁴⁾. As the thickness of the slice increases, the proportions of scatter and backscatter radiation increases. So, it is also expected that the dose value at the center of slice thickness will increase, but this effect is not as large as the effect of photon energy (figure 4).

Our study shows that the contributions to scattered radiations in the dose profile are much higher than in primary beams. According to Boone ⁽¹⁵⁾, the scattering dose profile was still significant when the beam width is smaller than 10 mm. There is little correlation between slice thickness and the dose value of the center of radiation fields ($R^2=0.58$). In most related studies, the relationship between scan length and dose profiles in the phantom was investigated. Increases in the scan length are associated with increases in the dose at the center of the slice. However, according to Dixon ⁽¹⁶⁾, it eventually reaches an equilibrium such that further increasing the scan length has no effect on the dose at the center of the slice.

In several studies, SPR values were calculated in the CT scan system inside a phantom ⁽¹⁾ or at the location of the detector arrays ⁽⁸⁾. In our study, SPR was investigated at the center of a PMMA phantom (figure 4). The area under the dose curve of the scattered beam was calculated by subtracting the primary radiation dose from the total dose profile. Figures 3 and 4 illustrate that primary beams are more strongly affected by the energy of the X-ray photons, and scattered radiations are more affected by slice thickness. The extent of the scattered photon distribution from the center of the radiation field is an important factor when estimating the patient dose during CT imaging (table 1).

In many studies, CTDI₁₀₀ is not suitable for expressing a dose index in a multi-slice CT scan where the X-ray beam width is wide and its use underestimates the patient dose value ^(15, 17-19). Several studies have attempted to find a way to increase the accuracy of CTDI measurements using long CT phantoms (up to 300 mm) and long ion chamber dosimeters ^(10, 19). These measurements are impractical due to the weight

and size of the phantoms. It is also difficult to make long ion chamber dosimeters, and such dosimeters are not readily available ⁽²⁰⁾. However, simulation methods make it easy to make accurate CTDI calculations.

Our study shows that for accurate CTDI estimations, the PMMA phantom must be approximately 700 mm long for a thickness of 5 mm and 80 kV of energy; it should be approximately 900 mm long for a thickness of 40 mm and 140 kV of energy. In Anam *et al.*'s ⁽²¹⁾ study, the scatter index (SI) parameter was introduced, and a dose profile of the X-ray beam in a 150 mm phantom in spiral mode with a 600-mm-long phantom was proposed for the appropriate estimation of CTDI. The findings were similar for the body CTDI phantom and head phantom (160 mm in diameter) ^(22, 23). Our study shows that the radiation dose of the scattered beams exists at a distance of more than 600 mm. We propose that the integral interval of ± 450 mm (figure 1C) is appropriate for CTDI calculations.

According to table 2, beyond 310 mm from the center of slice thickness, there is no significant difference between the dose of the maximum photon energy (140 kV) and the minimum energy (80 kV) at a slice thickness of 40 mm. It is, therefore, reasonable to investigate the effect of CT scan imaging technical factors on the dose in the PMMA phantom up to 310 mm from the center of the phantom. The use of a phantom that is 620 mm in length seems to be sufficient to study the influence of technical factors on the dose profile of scattered photons.

CONCLUSION

Our study shows that increasing the slice thickness results in a significant decrease in the SPR value. Primary beams are more strongly affected by the energy of the photons, and scatter beams are more affected by slice thickness for a 64-slice multi-detector CT scan system. Thus, the PMMA phantom length should be between 700 and 900 mm to achieve accurate CTDI estimations.

Conflicts of interest: Declared none.

REFERENCES

1. Boone JM (2009) Dose spread functions in computed tomography: A Monte Carlo study. *Med Phys*, **36(10)**: 4547-4554.
2. Dixon RL and Ballard AC (2007) Experimental validation of a versatile system of CT dosimetry using a conventional ion chamber: Beyond CTDI100. *Med Phys*, **34(8)**: 3399-3413.
3. Bauhs AJ, Vrieze TJ, Primak AN, et al. (2008) CT dosimetry: comparison of measurement techniques and devices. *Radio Graphics*, **28(1)**: 245-253.
4. National Council on Radiation Protection and Measurements (2009) Ionizing radiation exposure of the population of the United States Report no. 160. Bethesda, Md: National Council on Radiation Protection and Measurements. http://www.ncrponline.org/Publications/Press_Releases/160press.html
5. Brenner DJ and Hall EJ (2007) Computed tomography an increasing source of radiation exposure. *N Engl J Med*, **357(22)**: 2277-84.
6. Mettler FA Jr, Thomadsen BR, Bhargavan M, et al. (2008) Medical radiation exposure in the U.S. in 2006: Preliminary results. *Health Phys*, **95(5)**: 502-507.
7. Tofts PS and Gore J C (1980) Some sources of artefact in computed tomography. *Phys Med Biol*, **25(1)**: 117-127.
8. Johns PC and Yaffe M (1982) Scattered radiation in fan beam imaging systems. *Med Phys*, **9(2)**: 231-239.
9. Akbarzadeh A, Ay MR, Ghadiri H, et al. (2010) Measurement of scattered radiation in a volumetric 64-slice CT scanner using three experimental Techniques. *Phys Med Biol*, **55(8)**: 2269-2280.
10. Geleijns J, Salvado Artells M, Bruin P W de, et al. (2009) Computed tomography dose assessment for a 160 mm wide, 320 detector row, cone beam CT scanner. *Phys Med Biol*, **54(10)**: 3141-3159.
11. Fallah Mohammadi Gh R, Riyahi Alam N, Geraily Gh, Paydar R (2016) Thorax organ dose estimation in computed tomography based on patient CT data using Monte Carlo simulation. *Int J Radiat Res*, **14(4)**: 313-321.
12. Shanmugasundaram S and Chandrasekaran S (2018) Optimization of variance reduction techniques used in EGSnrc Monte Carlo codes. *Journal of Medical Physics*, **43(3)**: 185-194.
13. Chow James CL and KLeung MK (2008) A graphical user interface for calculation of 3D dose distribution using Monte Carlo simulations. *Journal of Physics: Conference Series* 102; 012003.
14. Percuoco R (2014) Plain radiographic imaging, in clinical imaging (Third edition), <https://www.sciencedirect.com/topics/medicine-and-dentistry/compton-scattering>.
15. Boone JM (2007) The trouble with CTDI₁₀₀. *Med Phys*, **34(4)**: 1364-1371.
16. Dixon RL, Munley MT and Bayram E (2005) An improved analytical model for CT dose simulation with a new look at the theory of CT dose. *Med Phys*, **32(12)**: 3712-3728.
17. Dixon RL (2003) A new look at CT dose measurement: Beyond CTDI. *Med Phys*, **30(6)**: 1272-1280.
18. Ruan C, Yukihara EG, Clouse WJ, et al. (2010) Determination of multi slice computed tomography dose index (CTDI) using optically stimulated luminescence technology. *Med Phys*, **37(7)**: 3560-3568.
19. Mori S, Endo M, Nishizawa K, et al. (2005) Enlarged longitudinal dose profiles in cone-beam CT and the need for modified dosimetry. *Med Phys*, **32(4)**: 1061-1069.
20. IAEA human health reports No. 5 (2011) Status of computed tomography dosimetry for wide cone beam scanners. International atomic energy agency Vienna. <http://www.iaea.org/Publications/index.html>.
21. Anam C, Haryanto F, Widita R, et al. (2017) Scatter index measurement using a CT dose profiler. *J Med Phys Biop*, **4(1)**: 95-102.
22. Anam C, Haryanto F, Widita R, Arif I, Dougherty G (2016) Profile of CT scan output dose in axial and helical modes using convolution. In *Journal of Physics: Conference Series* (Vol. 694, No. 1, p. 012034). IOP Publishing.
23. Liu M, Wang Y, Liao X (2015) Computed tomography dose index measurement for Hi-ART mega voltage helical CT. *Radiation Protection Dosimetry*, **17(3)**: 1-5.